Journal of Constructional Steel Research 66 (2010) 897–905

Contents lists available at ScienceDirect

Journal of Constructional Steel Research

journal homepage: www.elsevier.com/locate/jcsr

Probabilistic analysis for design assessment of continuous steel–concrete composite girders

Alessandro Zona [a,*], Michele Barbato [b], Andrea Dall'Asta [a], Luigino Dezi [c]

[a] Department PROCAM, University of Camerino, Viale della Rimembranza, 63100, Ascoli Piceno, Italy

[b] Department of Civil and Environmental Engineering, Louisiana State University, 3531 Patrick F. Taylor Hall, Baton Rouge, LA 70803, USA

[c] Department of Architecture, Constructions and Structures, Marche Polytechnic University, Via Brecce Bianche 60131, Ancona, Italy

ARTICLE INFO

Article history:
Received 31 August 2009
Accepted 22 January 2010

Keywords:
Steel–concrete composite bridges
Probabilistic response analysis
Response sensitivity analysis
Nonlinear finite element analysis
Partial interaction
Plastic design
Safety format

ABSTRACT

In the design of continuous steel–concrete composite girders, cross section plastic resistance can be exploited in the sagging regions, where the compressed flange of the steel beam is connected to the reinforced concrete slab. However, elastic verification of cross sections is normally adopted in the hogging regions, where the compressed portion of the steel beam is unrestrained by the concrete slab and more prone to buckling. In a combined design approach, which uses the cross section plastic resistance in the sagging regions and the cross section elastic resistance in the hogging regions, the design must satisfy the condition that the sagging plastic moment can develop while the hogging bending moment remains below the elastic limit. The objectives of this work are to present a framework for simplified probabilistic nonlinear analysis of steel–concrete composite bridges and to assess, through such framework, the combined elastic–plastic design as applied to a realistic three-span continuous steel–concrete composite road bridge. The methodology presented here is based on the First-Order Second-Moment (FOSM) approximation, adopted to compute the first- and second-order statistical moments (means, variances and covariances) of structural response quantities. Deterministic and probabilistic numerical results for the benchmark problem are illustrated and discussed.

1. Introduction

Continuous steel–concrete composite (SCC) girders are used extensively for the construction of short and medium span bridges, due to the benefits derived from the combination of structural steel and reinforced concrete, as well as from span continuity [1,2]. Solutions of high structural and aesthetic value can be obtained, provided that the necessary attention is given to design and construction phases [3]. The structural behavior of SCC beams for buildings and bridges is influenced by a considerable number of parameters describing sagging and hogging sections, layout of spans, and load patterns. In the past, various authors dealt with design aspects (e.g., [4–12]), recognizing some issues in the flexural design of continuous composite systems.

In the sagging regions, where the compressed flange of the steel beam is connected to the reinforced concrete slab, the cross sections generally belong to class 1 or class 2 (compact sections), according to the Eurocodes [13,14]. Therefore, design bending resistance can be determined by rigid-plastic theory [13,14]. Thus, a considerable reduction of the steel weight can be obtained compared to a design based on the elastic bending resistance. In the hogging regions, where the compressed portion of the steel beam is unrestrained by the concrete slab and more prone to buckling, the cross sections commonly belong to class 3 or class 4 (slender sections) and have insufficient ductility for plastic design. Thus, elastic analysis is adopted for calculating the design bending resistance in the hogging regions [13,14]. This design approach, which uses the cross section plastic resistance in the sagging regions and the cross section elastic resistance in the hogging regions, is referred to as combined design. The combined design must satisfy the condition that the sagging plastic bending moment can develop while the hogging bending moment remains below the elastic limit. In order to verify that this condition is satisfied, nonlinear analysis can be used. Since multi-span continuous girders with variable cross section geometry are common in real-world designs and many loadings conditions must be considered, an efficient numerical procedure for nonlinear analysis is necessary. Such procedure should also include the deformability and nonlinear behavior of shear connectors between reinforced concrete slab and steel beam, as explicitly requested by Eurocode 4 Part 1 [13] and Part 2 [14].

Nevertheless, uncertainties in material properties, geometry, and several other modelling parameters that are stochastic

* Corresponding author. Tel.: +39 0736 249680; fax: +39 0736 249672.
E-mail address: alessandro.zona@unicam.it (A. Zona).

0143-974X/$ – see front matter © 2010 Elsevier Ltd. All rights reserved.
doi:10.1016/j.jcsr.2010.01.015

quantities in nature influence the response analysis results. Unfavorable combinations of such random parameters might endanger the actual fulfilment of the hypothesis at the base of the combined design approach (i.e., hogging regions below the elastic limit and sufficient ductility in the sagging regions). Therefore, in addition to an accurate deterministic model, a methodology is needed to propagate uncertainties from the parameters defining the model of the structure to the structural response quantities of interest.

In this work, comparisons are made between the design criterion for continuous SCC bridge girders based entirely on elastic resistance of cross sections (elastic design), and the design criterion based on plastic resistance of sagging cross sections and elastic resistance of hogging cross sections (combined design). In particular, this paper considers the elastic and combined designs of a realistic three-span continuous SCC road bridge. The designs of this bridge were obtained according to the Eurocodes. Finite element (FE) probabilistic nonlinear response analysis, based on the First-Order Second-Moment (FOSM) approximation [15], is used to evaluate behavioral aspects and safety levels of these two designs. Deterministic and probabilistic results are illustrated and discussed. Although applied here to a specific problem, the probabilistic response analysis methodology presented in this paper is general and can be applied to design of SCC bridges based also on design codes other than the Eurocodes.

2. Nonlinear probabilistic analysis of SCC girders

2.1. Introductory remarks

Probabilistic response analysis consists of computing the probabilistic characterization of the response of a specific structure. This analysis requires the probabilistic characterization of material, geometric, and loading parameters as input. Several methods are available for probabilistic response analysis [15]. Among these methods, Monte Carlo Simulation (MCS) [16] is perhaps the most widely used. The MCS procedure requires: (1) generation of N realizations of the n-dimensional random parameter vector $\boldsymbol{\Theta}$ according to a given n-dimensional joint Probability Density Function (PDF); (2) computation by FE response analysis of N response curves for each component of the m-dimensional response vector $\mathbf{R}$, corresponding to the N realizations of the random parameter vector $\boldsymbol{\Theta}$; (3) statistical estimation of specified marginal and joint moments of the components of $\mathbf{R}$ at each load step. MCS is a general and robust methodology, but suffers from the two following significant limitations. First, MCS requires complete knowledge of the joint PDF of the random parameters $\boldsymbol{\Theta}$, for which, in general, only partial information is available. Second, MCS requires performing N FE response analyses. This number N can be very large for accurate estimates of marginal and joint moments of response quantities $\mathbf{R}$, and increases rapidly with the order of the statistical moments. For realistic bridge structures, complex nonlinear FE analyses are necessary for accurate prediction of the structural response, and repeating such analyses a large number of times could be computationally prohibitive.

2.2. FOSM approximation for probabilistic response analysis

An approximate method of probabilistic response analysis is the FOSM method [15], in which mean values (first-order statistical moments), variances and covariances (second-order statistical moments) of the response quantities are estimated from the first-order Taylor series expansion of the response vector $\mathbf{R}$. Given the vector of n random parameters $\boldsymbol{\Theta}$, the corresponding mean values vector $\boldsymbol{\mu}_{\boldsymbol{\Theta}}$ and covariance matrix $\boldsymbol{\Sigma}_{\boldsymbol{\Theta}}$ are

$$\left[\boldsymbol{\mu}_{\boldsymbol{\Theta}}\right]_i = \mu_i \quad (i = 1, 2, \ldots, n) \tag{1}$$

$$\left[\boldsymbol{\Sigma}_{\boldsymbol{\Theta}}\right]_{ij} = \rho_{ij}\sigma_i\sigma_j \quad (i, j = 1, 2, \ldots, n) \tag{2}$$

where μ_i and σ_i denote respectively the mean value and the standard deviation of random parameter Θ_i, while ρ_{ij} is the correlation coefficient of random parameters Θ_i and Θ_j ($\rho_{ii} = 1$; $i = 1, 2, \ldots, n$). The linearization of the response vector $\mathbf{R}$ by means of the first-order truncation of its Taylor series expansion in the random parameters $\boldsymbol{\Theta}$ about a given point $\boldsymbol{\theta}_0$, gives:

$$\mathbf{R}(\boldsymbol{\Theta}) \approx \mathbf{R}_{\text{lin}}(\boldsymbol{\Theta}) = \mathbf{r}(\boldsymbol{\theta}_0) + \nabla_{\boldsymbol{\theta}}\mathbf{r}|_{\boldsymbol{\theta}=\boldsymbol{\theta}_0}(\boldsymbol{\Theta} - \boldsymbol{\theta}_0) \tag{3}$$

in which

$$\left[\nabla_{\boldsymbol{\theta}}\mathbf{r}|_{\boldsymbol{\theta}=\boldsymbol{\theta}_0}\right]_{ij} = \frac{\partial r_i}{\partial \theta_j} \quad (i = 1, 2, \ldots, m, \text{ and } j = 1, 2, \ldots, n) \tag{4}$$

is the sensitivity of response quantity r_i to parameter θ_j evaluated at $\boldsymbol{\theta} = \boldsymbol{\theta}_0$ [17], and lower case letters $\boldsymbol{\theta}$ and $\mathbf{r}$ denote specific realizations of the corresponding random quantities indicated with the upper case letters $\boldsymbol{\Theta}$ and $\mathbf{R}$. Using the Mean-Centered FOSM method, the vector $\mathbf{R}$ is approximated by a first-order truncation of its Taylor series expansion in the random parameters $\boldsymbol{\Theta}$ about their mean values $\boldsymbol{\mu}_{\boldsymbol{\Theta}}$ as

$$\mathbf{R}(\boldsymbol{\Theta}) \approx \mathbf{R}_{\text{lin}}(\boldsymbol{\Theta}) = \mathbf{r}\left(\boldsymbol{\mu}_{\boldsymbol{\Theta}}\right) + \nabla_{\boldsymbol{\theta}}\mathbf{r}|_{\boldsymbol{\theta}=\boldsymbol{\mu}_{\boldsymbol{\Theta}}}\left(\boldsymbol{\Theta} - \boldsymbol{\mu}_{\boldsymbol{\Theta}}\right). \tag{5}$$

The first- and second-order statistical moments of the response quantities $\mathbf{R}$ are approximated by the corresponding moments of the linearized response quantities, i.e.,

$$\begin{aligned}\boldsymbol{\mu}_{\mathbf{R}} &\approx \boldsymbol{\mu}_{\mathbf{R}_{\text{lin}}} = \mathrm{E}\left[\mathbf{R}_{\text{lin}}(\boldsymbol{\Theta})\right] \\ &= \mathbf{r}\left(\boldsymbol{\mu}_{\boldsymbol{\Theta}}\right) + \nabla_{\boldsymbol{\theta}}\mathbf{r}|_{\boldsymbol{\theta}=\boldsymbol{\mu}_{\boldsymbol{\Theta}}}\mathrm{E}\left[\boldsymbol{\Theta} - \boldsymbol{\mu}_{\boldsymbol{\Theta}}\right] = \mathbf{r}\left(\boldsymbol{\mu}_{\boldsymbol{\Theta}}\right)\end{aligned} \tag{6}$$

$$\begin{aligned}\boldsymbol{\Sigma}_{\mathbf{R}} &\approx \boldsymbol{\Sigma}_{\mathbf{R}_{\text{lin}}} = \mathrm{E}\left[\left(\mathbf{R}_{\text{lin}}(\boldsymbol{\Theta}) - \boldsymbol{\mu}_{\mathbf{R}_{\text{lin}}}\right)\left(\mathbf{R}_{\text{lin}}(\boldsymbol{\Theta}) - \boldsymbol{\mu}_{\mathbf{R}_{\text{lin}}}\right)^T\right] \\ &= \nabla_{\boldsymbol{\theta}}\mathbf{r}|_{\boldsymbol{\theta}=\boldsymbol{\mu}_{\boldsymbol{\Theta}}}\boldsymbol{\Sigma}_{\boldsymbol{\Theta}}\left(\nabla_{\boldsymbol{\theta}}\mathbf{r}|_{\boldsymbol{\theta}=\boldsymbol{\mu}_{\boldsymbol{\Theta}}}\right)^T\end{aligned} \tag{7}$$

in which $\mathrm{E}[\cdots]$ denotes the mathematical expectation operator [18].

The explicit forms of variances and covariances of the response quantities considered are derived from Eq. (7) as follows:

$$\begin{aligned}\sigma^2_{R_k} &\approx \sum_{i=1}^{n}\left(\left.\frac{\partial r_k}{\partial \theta_i}\right|_{\boldsymbol{\theta}=\boldsymbol{\mu}_{\boldsymbol{\Theta}}}\sigma_i\right)^2 \\ &\quad + 2\sum_{i=1}^{n}\sum_{j=1}^{i-1}\rho_{ij}\left.\frac{\partial r_k}{\partial \theta_i}\right|_{\boldsymbol{\theta}=\boldsymbol{\mu}_{\boldsymbol{\Theta}}}\left.\frac{\partial r_k}{\partial \theta_j}\right|_{\boldsymbol{\theta}=\boldsymbol{\mu}_{\boldsymbol{\Theta}}}\sigma_i\sigma_j \quad (k = 1, \ldots, m)\end{aligned} \tag{8}$$

$$\begin{aligned}\operatorname{cov}[R_k, R_s] &\approx \sum_{i=1}^{n}\sum_{j=1}^{n}\rho_{ij}\left.\frac{\partial r_k}{\partial \theta_i}\right|_{\boldsymbol{\theta}=\boldsymbol{\mu}_{\boldsymbol{\Theta}}}\left.\frac{\partial r_s}{\partial \theta_j}\right|_{\boldsymbol{\theta}=\boldsymbol{\mu}_{\boldsymbol{\Theta}}}\sigma_i\sigma_j \\ &\quad (k, s = 1, \ldots, m)\end{aligned} \tag{9}$$

respectively, being R_k and R_s the k-th and s-th components of $\mathbf{R}$.

Eqs. (6) and (7) provide information on the variability of the response due to the uncertainty of the modelling parameters and on the statistical correlation between the different response quantities. These approximate first- and second-order response statistics can be readily obtained when response sensitivities evaluated at the mean values of the random parameters are available. Such response sensitivities can be computed by the very efficient and accurate Direct Differentiation Method (DDM) [17,19–21]. FOSM-based probabilistic response analysis, in conjunction with DDM for response sensitivity calculations, has a low additional computational cost as compared to a deterministic-only nonlinear response analysis. The FOSM method requires statistical information on the

uncertain parameters that are usually available (i.e., the first- and second-order statistical moments in Eqs. (1) and (2)). In addition, the FOSM approximation was found sufficiently accurate in estimating mean and standard deviation of response quantities of random structural systems under quasi-static loads, when structural response nonlinearities are in the low-to-moderate range [22,23]. For the above reasons, the DDM-based FOSM method can conveniently be applied as an efficient and practical method for probabilistic analysis of bridge structures as opposed to MCS or other more advanced methods. In fact, these methods require larger computational efforts and higher-order statistical information, which is only rarely available.

2.3. Response and response sensitivity analysis of SCC beams

A simple and effective two-dimensional 10 nodal degrees-of-freedom (DOF) displacement-based composite beam finite element with deformable shear connection (partial interaction) [24] is used in this study. Its formulation is based on the following assumptions: (i) the Euler–Bernoulli beam theory (in small deformations) applies to both components of the composite beam, and (ii) the deformable shear connection is represented by an interface model with distributed bond allowing interlayer slip and enforcing contact between the steel and concrete components. Such FE model includes reinforced concrete and steel nonlinear behavior, as well as the deformability and nonlinear behavior of shear connectors between reinforced concrete slab and steel beam, as explicitly requested by Eurocode 4 Part 1 [13] and Part 2 [14]. This 10DOF finite element was proven to produce accurate results for the nonlinear analysis of SCC beams [25] and SCC beams with external prestressing [26], as well as for SCC frames under cyclic loads [27]. Material nonlinearity-only is considered since geometric nonlinearities do not have any practical effect in realistic non-prestressed steel–concrete continuous girders [28]. The 10DOF composite beam element was augmented with response sensitivity calculations by means of the DDM [29,30]. In the DDM, the consistent response sensitivities are computed at each analysis step after convergence of the response computation. This requires an exact differentiation of the FE algorithm for response calculation (including the numerical integration scheme for the material constitutive law) with respect to each sensitivity parameter θ. Consequently, the response sensitivity calculation algorithm affects the various hierarchical layers of FE response simulation, namely: (1) structure level, (2) element level, (3) section (integration point) level and (4) material level. A detailed description of the DDM procedure as applied to displacement-based FEs for composite beams with deformable shear connection can be found in [29], where specific issues for elements with internal nodes are also illustrated. Results of the DDM derivation and computer implementation for SCC beams were validated [29–31] using the Forward Finite Difference (FFD) method (i.e., estimating the derivative of the response by imposing a perturbation of the sensitivity parameter θ and using a first-order finite difference approximation [17]). In addition, probabilistic nonlinear response results for SCC beams with deformable shear connection obtained by DDM-based FOSM analysis were validated [32] by comparisons with MCS.

2.4. Material models for response and response sensitivity analysis of SCC beams

Material constitutive models for response and response sensitivity analysis are required to compute the stress resulting from a given strain history, as well as the derivative of the stress with respect to the material parameters assumed as uncertain in the probabilistic analysis. The constitutive material models adopted in this study are hereafter briefly illustrated, together with the uncertain modelling parameters and the relevant response sensitivity computations. Cyclic constitutive models are used for steel and concrete materials and for the shear connection. Thus, the framework presented here can be employed without modification for both monotonic/cyclic static loading and dynamic loading.

The constitutive law used for the steel of the beam and for the reinforcing steel in the concrete slab is the uniaxial Menegotto–Pinto constitutive model [33], a nonlinear law capable of modelling both kinematic and isotropic hardening [34], as well as the Bauschinger effect. A typical cyclic response of the steel material model is shown in Fig. 1(a). The constitutive parameters assumed as random parameters (i.e., the components of the vector $\boldsymbol{\Theta}$ related to the steel materials) are the modulus of elasticity, E, the yield stress, f_y, and the post-yield to initial tangent stiffness ratio b. Details on the model, its numerical implementation, and response sensitivity computation can be found in [35].

The selected constitutive law for the concrete material in compression is a uniaxial cyclic law with monotonic envelope given by the Popovics–Saenz law [36]. The constitutive parameters modelled as random variables are the compressive strength, f_c, the initial tangent stiffness, E_c, the strain at compressive strength, ε_p, the softening stress at the inflection point, f_0, and the strain corresponding to the softening stress, ε_0 (Fig. 1(b)). In order to satisfy Eurocode prescriptions, as illustrated in the following paragraph, null strength is assumed for the concrete in traction. The details of the formulation of this constitutive law and related response sensitivity computation can be found in [31].

The behavior of the shear connectors is described by a force–slip (f_s-slip) cyclic model with monotonic envelope given by the Ollgaard et al. law [37]. The cyclic response of the shear connectors is based on a simplified phenomenological description of experimental tests. A typical cyclic response of the shear connection model is shown in Fig. 1(c). The constitutive parameter modelled as a random variable is the shear strength, f_{smax}. The details of this constitutive law and related response sensitivity computations can be found in [31].

In order to compute the FOSM approximations of the mean response vector (Eq. (6)) and response covariance matrix (Eq. (7)), mean values, standard deviations, and correlation coefficients are needed for all material parameters modelled as random variables.

2.5. Nonlinear analysis and safety format in the Eurocodes

Eurocode 4 Part 2 [14] (Paragraph 5.4.3 on nonlinear global analysis for bridges) allows nonlinear analysis and specifically requires that the behavior of the shear connection shall be taken into account. More information is found in Eurocode 4 Part 1 [13] (Paragraph 5.4.3 on nonlinear global analysis), which allows nonlinear analysis in accordance with Paragraph 5.7 of Eurocode 2 Part 1-1 [38] and Paragraph 5.4.3 of Eurocode 3 Part 1 [39].

In paragraph 5.7 of Eurocode 2 Part 1-1, nonlinear analysis is allowed for both ultimate limit states and service limit states, and various basic indications are given. Eurocode 3 Part 1 (paragraph 5.4.3 on plastic global analysis) requires that plastic global analysis should only be used where the stability of members at plastic hinges can be assured. Indications on steel models for plastic global analysis are also given, allowing the use of several different models. These models range from simplified plastic models (e.g., bilinear stress–strain with hardening), to more realistic stress–strain relationships (e.g., true stress–strain curves derived from test results).

In addition, paragraph 5.7 of Eurocode 2 Part 2 [40] allows nonlinear analysis, provided that the model can appropriately cover all failure modes and that the concrete tensile strength is not utilized as a primary load resisting mechanism. The same paragraph 5.7 of

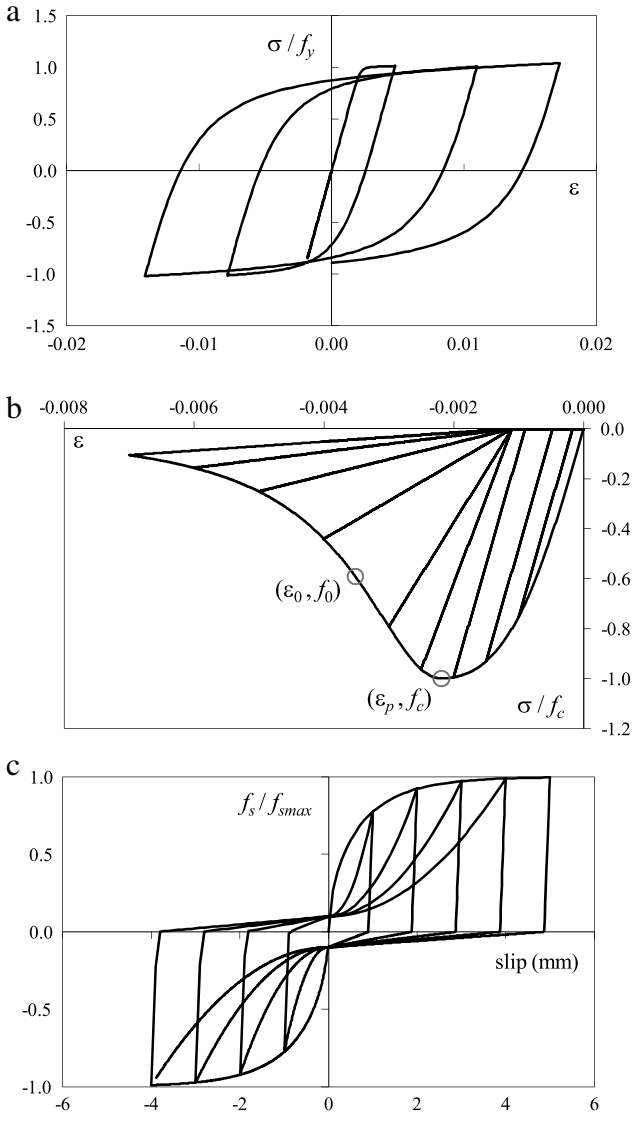

Fig. 1. Typical cyclic responses for material constitutive models: (a) stress–strain for structural steel and reinforcements; (b) stress–strain for concrete; (c) force–slip for shear connection.

Eurocode 2 Part 2 recommends suitable stress–strain relationships for concrete and reinforcement steel, as well as a safety format that is illustrated hereafter.

This safety format for nonlinear analysis is subdivided into the following steps:

Step 1: The resistance should be evaluated for different levels of appropriate actions, which should be increased from their serviceability values by incremental steps, so that the value of $\gamma_G G_k$ and $\gamma_Q Q_k$ are reached in the same step. Here, G_k and Q_k denote the characteristic values of permanent and variable actions, respectively; γ_G and γ_Q are the partial factors for permanent and variable actions, respectively. In bridge structures, $\gamma_G = \gamma_Q = 1.35$ in locations where loads are unfavorable, $\gamma_G = 1.00$ and $\gamma_Q = 0$ where loads are favorable [41].

Step 2: The incremental loading process should be continued until one region of the structure attains the ultimate strength, or there is global failure of the structure. The corresponding load is referred to as q_{ud}.

Step 3: An overall safety factor γ_O should be applied to obtain the corresponding resistance $R(q_{ud}/\gamma_O)$ under load q_{ud}/γ_O.

Step 4: The following inequality should be satisfied:

$$E\left(\gamma_G G_k + \gamma_Q Q_k\right) \leq R\left(\frac{q_{ud}}{\gamma_{Rd}\gamma_O}\right) \tag{10}$$

where $E(X)$ is the effect of action X, $\gamma_O = 1.20$ is the overall safety factor, and $\gamma_{Rd} = 1.06$ is the partial factor for model uncertainty for resistance (uncertainty in the resistance model plus geometric deviations if not modelled explicitly, as clarified in Annex C of Eurocode 0 [41]).

3. Probabilistic analysis of a three-span continuous SCC girder

3.1. Elastic design and combined design of the SCC girder

A realistic three-span continuous SCC road bridge is considered as the benchmark problem in this work (Fig. 2). Two bridge design solutions, obtained according to the Eurocodes, are studied: the first solution is based on cross section elastic resistance (elastic design), while the second one is based on cross section plastic resistance in the sagging regions and cross section elastic resistance in the hogging regions (combined design). As already noted, in the sagging regions the cross sections generally belong to class 1 or class 2 (compact sections) and design bending resistance can be determined by rigid-plastic theory [13,14]. However, in the hogging regions the cross sections commonly belong to class 3 or class 4 (slender sections) and have insufficient ductility for plastic design. Thus, in the hogging regions, elastic analysis is adopted for calculating the design bending resistance [13,14].

The bridge cross section is made of twin I-beams of steel S355 connected to a reinforced concrete slab of concrete f_{ck} 30 MPa (characteristic compressive strength) with reinforcements f_{yk} 430 MPa (characteristic yield stress). The steel beams are connected to each other with a transverse IPE 700 beam every 8.00 m. The actions considered for the design are permanent loads [42], wind loads [43], temperature changes [44], concrete shrinkage [14], and road traffic loads due to Load Model 1 [45]. A preliminary continuous beam model was studied using linear analysis according to Eurocode 4 Part 2 [14]. The envelopes of bending moment and shear force along the bridge axis were obtained from the combination of the applied actions with their relevant load amplification factors [41]. From such envelopes, both the elastic and the combined design were derived. Specifically, in the elastic design, the steel beam cross sections were dimensioned to grant the least required elastic resistance under the sagging bending moments and under the hogging bending moments. Afterward, the continuous beam model was updated and reanalyzed, and the updated bending moment and shear force envelopes were used for the structural elastic verifications according to Eurocode 4 Part 2 [14]. In particular, the design considered ultimate limit state and service limit state elastic verifications under short-term and long-term conditions of the normal and shear stress in the steel beam, as well as of the normal stress in the concrete slab and reinforcements. Verifications of the stages of construction [14] and limitation of web breathing [46] were also included. The same framework was adopted for the combined design, with the difference that the steel beam cross sections in the sagging regions were dimensioned to grant the least required plastic resistance under the sagging bending moments. Accordingly, the structural verifications of the sagging cross sections in the combined design were based on the plastic limit state, according to Eurocode 4 Part 2 [14].

The elastic design and the combined design differ in flange and web thickness, as reported in Fig. 3. The upper and lower flange widths were kept constant in both design with values of 700 mm and 1000 mm, respectively. For both designs, the resulting cross

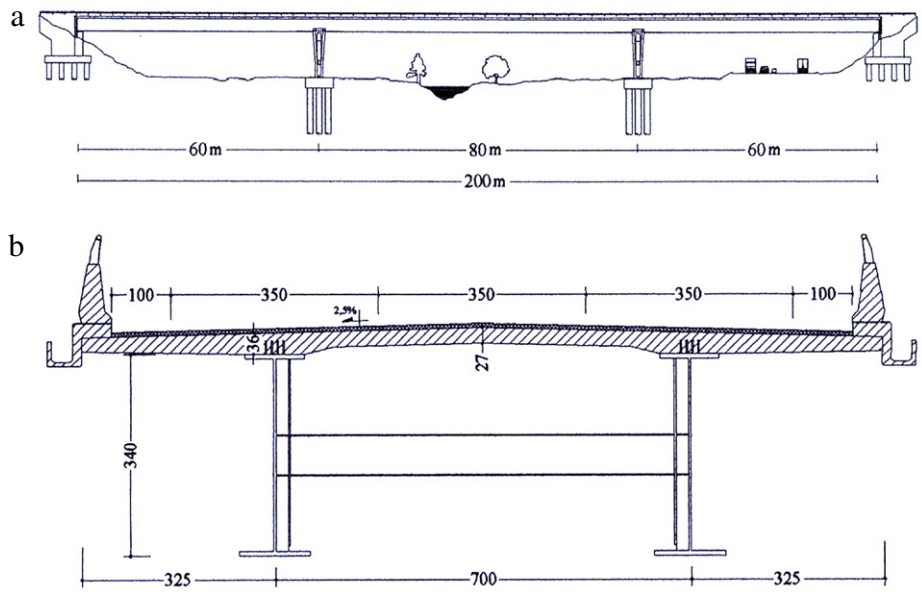

Fig. 2. Three-span continuous SCC girder used as benchmark problem: (a) longitudinal profile; (b) cross section (dimensions in cm except as otherwise specified).

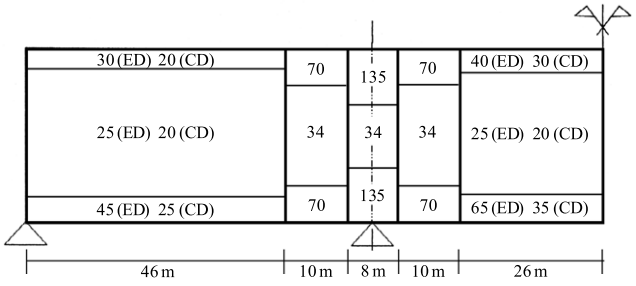

Fig. 3. Flanges and web thickness in the elastic design (ED) and in the combined design (CD) for half bridge (dimensions in mm except as otherwise specified).

Table 1
Material constitutive parameters modelled as uncertain and corresponding mean values and coefficients of variation (COV).

Material	Parameter	Mean	COV
Steel	f_y ($t \leq 40$ mm)	355 MPa	0.106
	f_y ($t > 40$ mm)	325 MPa	0.106
	E_0	200 000 MPa	0.033
	b	0.01	0.15
Concrete	f_c	25.29 MPa	0.20
	E_c	32 000 MPa	0.20
	ε_p	0.002	0.20
	f_0	15 MPa	0.20
	ε_0	0.004	0.20
Reinforcements	f_y	473 MPa	0.106
	E_0	200 000 MPa	0.033
	b	0.01	0.15
Shear connection	f_{smax} (segments S1)	5843 kN/m	0.20
	f_{smax} (segments S2)	4681 kN/m	0.20
	f_{smax} (segments S3)	3520 kN/m	0.20

sections are class 1 in the sagging regions and class 3 in the hogging regions. In the combined design, the weight of the twin I-beams' steel is 21.81% lower than it is in the elastic design. The reduction in the total weight of the composite girder is less significant (i.e., 3.95%) because the same reinforced concrete slab is used. In fact, the slab geometry depends on the transverse behavior, which is the same in the two designs.

Full shear connection between reinforced concrete slab and steel girder is provided by ductile shear connectors (i.e., with characteristic slip capacity of at least 6 mm [13,14]) with designed shear strength per unit length, f_{smax}, given in Table 1. Segments S1 correspond to the hogging regions from 46 to 70 m and 130 to 154 m, segments S2 are the sagging regions from 21 to 46 m and 154 to 179 m, and segments S3 are the sagging regions from 0 to 21 m, 70 to 130 m, and 179 to 200 m. Partial shear connection was not considered, as it is not allowed in bridge design [13,14].

3.2. Model and analysis assumptions

The effective width of the reinforced concrete slab was assumed as constant and equal to its full width. Since the traffic loads have a non-symmetric transverse configuration, only the more loaded side of the cross section (i.e., one steel I-beam connected to half width of the reinforced concrete slab) was analyzed as a planar composite beam. The composite beam axis was discretized into 38 FEs, i.e., 11 FEs for the lateral spans and 16 FEs for the central span, with an appropriate subdivision in order to accommodate variations in the cross section and shear connection strength. The finite elements used were the 10DOF beam elements with deformable shear connection [24] described in Section 2.3. The composite beam cross sections were modelled using a fiber-section discretization [24,29,30]. Vertical deflection was restrained at the four supports, while the horizontal displacement of the steel beam was restrained at the first support only. The characteristic values of the permanent loads, acting along the composite beam as vertical distributed loads, are: (1) the steel beam self weight, derived from its cross section area assuming 78.50 kN/m^3 as steel characteristic weight per unit volume; (2) the half slab uniform self weight equal to 50.20 kN/m; and (3) the superimposed permanent loads (road pavement and parapets) equal to 22.13 kN/m. The traffic loads acting along the composite beam were modelled as a uniform vertical load equal to 32.00 kN/m and two vertical forces equal to 385.00 kN travelling at a constant distance of 2.00 m from each other.

Nonlinear FE response analyses were performed by incrementing simultaneously dead and road traffic loads, according to the Eurocode load sequence previously described in Section 2.5. The load control incremental procedure was used together with the Newton–Raphson iterative method. The criterion adopted for terminating the nonlinear FE analyses was the attainment of the ultimate strain along any of the material fibers or of the ultimate

Table 2
Correlation coefficients for concrete material parameters.

Parameter	f_c	E_c	ε_p	f_0	ε_0
f_c	1.0	0.2	0.0	0.8	0.0
E_c	0.2	1.0	0.2	0.0	0.0
ε_p	0.0	0.2	1.0	0.0	0.8
f_0	0.8	0.0	0.0	1.0	0.0
ε_0	0.0	0.0	0.8	0.0	1.0

slip along the shear connection. In the load cases considered in this study, the FE analyses were always terminated due to the attainment of the ultimate strain of the steel (i.e., $\varepsilon_{su} = 0.01$). The shear connection slip remained always under 6 mm, while no limits were assumed for the concrete strain, since the concrete constitutive model is characterized by a softening branch after peak strength with stress decaying to zero. Since the cross sections at the hogging regions (class 3) cannot develop plastic deformations, the results obtained from the FE analyses were limited afterward, as described in the discussion of the numerical results. DDM-based response sensitivity analysis was performed simultaneously to the FE response analysis. FE response sensitivities were computed at the end of each load step increment, after convergence of the response was achieved. Data from response and response sensitivity analyses were subsequently post-processed using Eq. (7) to obtain variances and covariances of the response quantities.

The mean values and coefficients of variation (COVs; i.e., ratio between the standard deviation and the mean value) of the material parameters modelled in this study as random variables are given in Table 1, where t denotes the nominal thickness of the steel element. The mean value of the yield stress of the girder steel was assumed equal to its nominal value [39,46]. The mean value of the yield stress of reinforcements was taken as $1.1f_{yk}$, as indicated in paragraph 5.7 of Eurocode 2 Part 2 [40]. The mean value of the concrete compressive peak strength was computed as suggested in paragraph 5.7 of Eurocode 2 Part 2 [40]; i.e., $\gamma_{cf}f_{ck}$ with $\gamma_{cf} = 1.1\gamma_S/\gamma_C = 0.843$, where $\gamma_S = 1.15$ and $\gamma_C = 1.5$ are the partial safety factors for reinforcement steel and concrete, respectively. The mean value of the shear connection strength was assumed to coincide with the nominal design value, as different indications are not given in the Eurocodes. The COVs were obtained from studies available in the literature for steel [47,48] and concrete [49], while the COV of the shear connection strength was taken equal to that of the concrete strength. This assumption was based on the hypothesis that the shear connection failure due to concrete crushing is the foremost source of uncertainty, and is consistent with results available in the literature [50]. The correlation coefficients of the steel parameters were assumed to be zero, according to available studies [48]. The correlation coefficients adopted for the concrete parameters are given in Table 2. These values were based on engineering judgment, to avoid unrealistic combinations of parameters that might lead to inconsistencies in the definition of the relevant concrete constitutive law. The correlation coefficients between concrete and steel constitutive parameters were considered to be zero, since the properties of the two different materials are statistically independent. The connection strength was assumed to be uncorrelated to other material parameters, since no reliable information is available. It is worth observing that the values of the correlation coefficients between different material parameters have a smaller influence on the results of the probabilistic response analysis [32] than the means and standard deviations of these material parameters. Thus, the assumptions made on the values of these coefficients have a small effect on the numerical solution presented hereafter.

All uncertain material parameters were modelled as random fields spatially fully correlated; i.e., each material parameter was modelled as a single random variable over the entire length of the SCC girder. More advanced modelling, including discretization of each random field into several random variables correlated through a more accurate spatial correlation function, was not pursued in this work because: (1) the information available was not sufficient to describe the actual spatial correlation between the random variables at different locations in the bridge, and (2) other studies [32] suggest that the effect of spatial correlation is relatively small compared to the effects of other assumptions (e.g., correlation coefficients between random variables and marginal distribution types), even if not negligible.

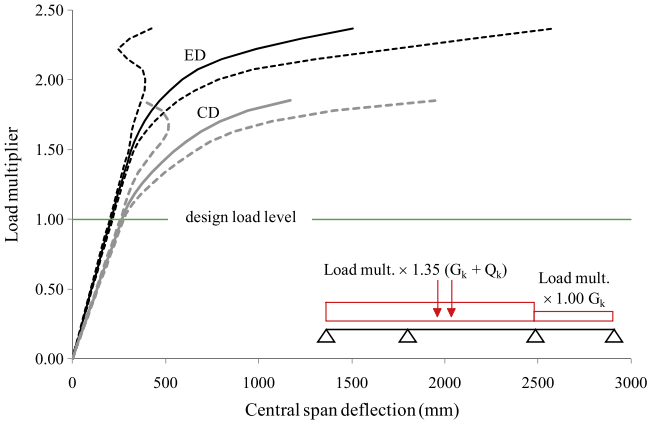

Fig. 4. Load multiplier versus mid-span deflection of the central span.

3.3. Numerical results

Selected results are shown for the load case which produces the maximum (negative) bending moment at the left intermediate support (see load pattern depicted in the inset of Fig. 4). Other load cases were considered and found less critical for the two bridge designs, and thus they are not reported in this paper for the sake of brevity.

Load–deflection curves for the two designs are shown in Fig. 4, where the applied load is represented in non-dimensional units by reporting the load multiplier (e.g., for the load multiplier equal to one, the applied loads are at the ultimate limit state design load level). The solid lines represent the mean deflection of the central span (computed via Eq. (6)), and the dashed curves represent the mean deflection plus/minus its standard deviation (computed via Eq. (7)). The dashed curves give a simple graphical indication of the dispersion of the results at the various load levels. As expected, the effect of uncertainties in the global response is limited for low load levels, and becomes much more pronounced when the structure undergoes significant plastic deformations. In fact, response sensitivities generally assume larger values as the SCC structure behavior becomes more nonlinear [29,30]. Both the elastic design (ED) and the combined design (CD) reach the design loads with an almost linear global behavior. Under design loads, the deflection COVs are 3.7% for the ED and 3.9% for the CD.

The sagging region of the central span deforms well beyond yielding, as shown by the moment–curvature curves in Fig. 5 and by the load–non-dimensional bending moment curves in Fig. 6. The non-dimensional bending moment is defined as the ratio between the bending moment M and the positive plastic moment $M_{pl,m}$ of the composite section, computed using rigid-plastic analysis based on the mean values of the material strengths, $M_{pl,m} = 136\,834$ kN m (ED) and $M_{pl,m} = 91\,548$ kN m (CD). Once again, the solid lines represent the mean response and the dashed curves represent the mean response plus/minus its standard deviation. The effect of uncertainties is small when

loads lower that the design load are considered (Fig. 6). For example, the bending moment COV is 0.98% (ED and CD) at the design load level. Plastic deformations are also attained at the left intermediate support, as seen in Fig. 7, in which the relevant moment–curvature curves (absolute values) are plotted. In this last case the moment–curvature relations for the two designs are almost coincident until the curve for the combined design ends at curvature 1.17×10^{-6} mm^{-1}. It is worth noting that the moment–curvature curves shown here are those derived from the nonlinear analysis of the whole bridge structure. Thus, they also include the effect of nonlinear partial interaction due to the actual evolution of slip gradients at the interface between slab and steel beam. These moment–curvature curves are considerably different from the curves obtained through a nonlinear analysis of the composite cross section based on the assumption of complete interaction, as observed in [51]. In addition, the moment–curvature curves considered here terminate when the nonlinear analysis ends due to global collapse, a condition that might occur before the ultimate curvature of the cross section is attained. It is also important to observe that the high-curvature region of the hogging moment–curvature curves in Fig. 7 were obtained from a finite element beam model that does not include local buckling. However, at the intermediate support, there is no sufficient ductility to develop plastic deformations, since the cross section belongs to class 3 in both bridge designs. Therefore, the ultimate limit state to be assumed in the nonlinear analysis presented here is the attainment of the elastic limit bending moment $M_{\mathrm{lim},el}$ (i.e., bending moment at yielding) in the hogging region. The presented probabilistic analysis gives the mean value $M_{\mathrm{lim},el,m}$ of $M_{\mathrm{lim},el}$ and the mean value plus/minus its standard deviation. Such values are represented by the horizontal lines in Fig. 7, while the vertical line indicates the curvature at $M_{\mathrm{lim},el,m}$. For both bridge designs, $M_{\mathrm{lim},el,m} = 169\,294$ kN m (absolute value) and its COV is 3.1% (i.e., the differences between ED and CD are negligible). The value of $M_{\mathrm{lim},el,m}$ and $M_{\mathrm{lim},el,m}$ plus/minus its standard deviation are depicted in Fig. 8 as the load–non-dimensional moment curves for the cross section at the intermediate support. The non-dimensional bending moment is defined here as the ratio between the bending moment M and $M_{\mathrm{lim},el,m}$. The intersection between the mean value of the demand (i.e., the computed mean bending moment at the intermediate support) and the mean value of the capacity (i.e., the mean elastic limit bending moment) is marked with a circle and identifies the load level corresponding to the attainment of the assumed ultimate limit state for a class 3 cross section. Such limit state load levels are indicated by "ED ULS m" (design load amplification = 1.925) and "CD ULS m" (design load amplification = 1.679), for the elastic and combined designs, respectively. The dashed curves and lines, again representing the relevant mean values plus/minus their standard deviation, give a simple indication of the dispersion of results.

A more conservative evaluation of the load level at the ultimate limit state can be computed by using the fractile 0.05 for the capacity and the fractile 0.95 for the demand. Assuming a lognormal distribution for the capacity, the fractile 0.05 of $M_{\mathrm{lim},el}$ is computed from its mean value and standard deviation [18], obtaining $M_{\mathrm{lim},el,005} = 160\,935$ kN m. Similarly, the fractile 0.95 of the bending moment, computed from the assumption of lognormal distribution for the demand, is depicted for both designs as a function of the load level in Fig. 9 (dashed curves), together with the mean response (solid curves). The intersection between $M_{\mathrm{lim},el,005}$ and the fractile 0.95 of the demand identifies the load level that corresponds to the attainment of the ultimate limit state when the characteristic values are considered instead of the mean values. Such limit state load levels are indicated by "ED ULS k" (design load amplification = 1.765) and "CD ULS k" (design load amplification = 1.520) for the elastic and combined designs,

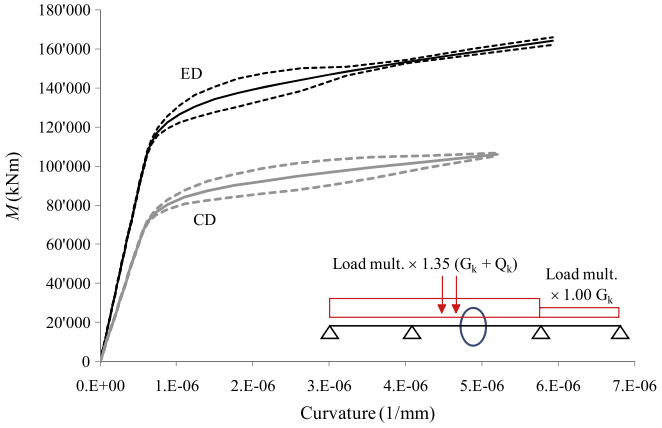

Fig. 5. Cross section at the central mid-span: Bending moment versus curvature.

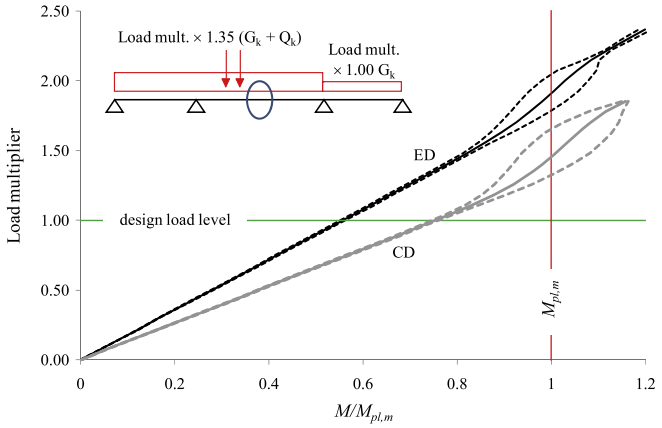

Fig. 6. Cross section at the central mid-span: Load multiplier versus non-dimensional bending moment.

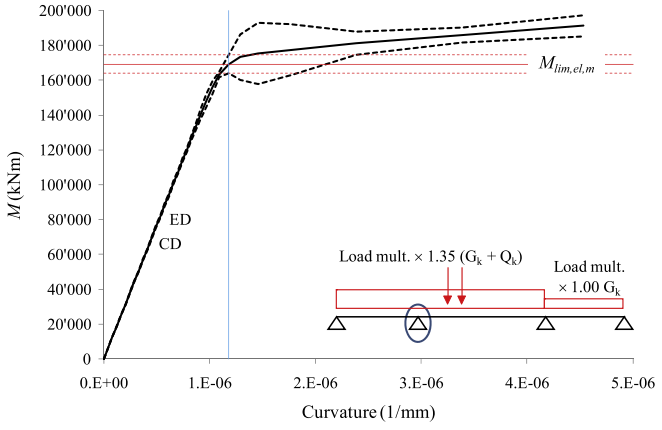

Fig. 7. Cross section at the left internal support: Bending moment versus curvature.

respectively, and are compared in Fig. 10 to the previously obtained limit state load levels. In both bridge designs, it is observed that the ultimate limit states are reached for load levels that are significantly higher than the design loads.

Characteristic values for the demand and the capacity are obtained under the assumption of lognormal distribution for the corresponding quantities. Such assumption is an approximation that becomes less accurate for higher nonlinearity [23]. Nevertheless, the ultimate state conditions are reached in correspondence with limited structural nonlinearity and response dispersion (as measured by the standard deviation). Thus the lognormal distribution can be considered an adequate approximation.

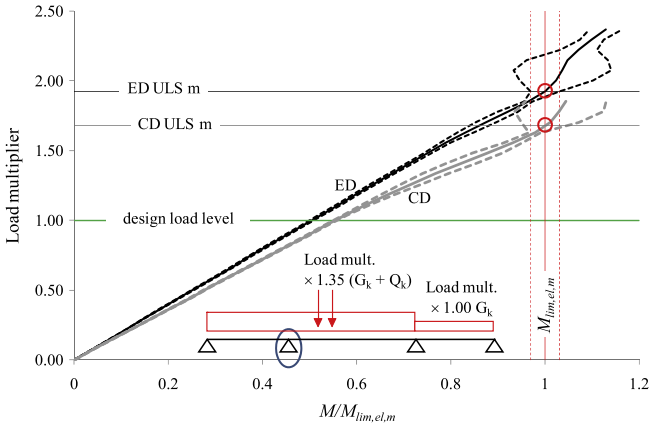

Fig. 8. Cross section at the left internal support: Load multiplier versus non-dimensional bending moment with marked limit states based on mean values.

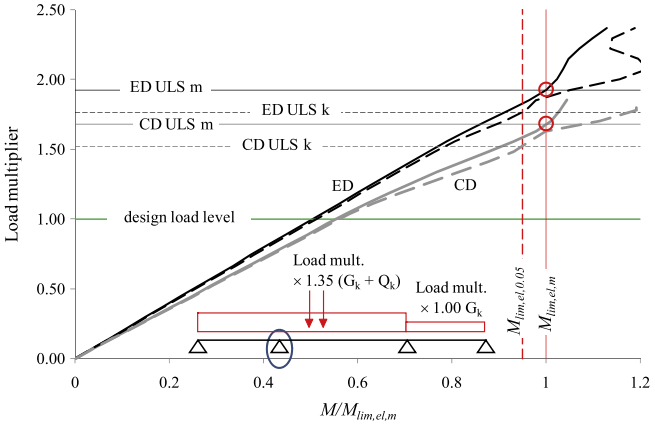

Fig. 9. Cross section at the left internal support: Load multiplier versus non-dimensional bending moment with marked limit states based on mean and characteristic values.

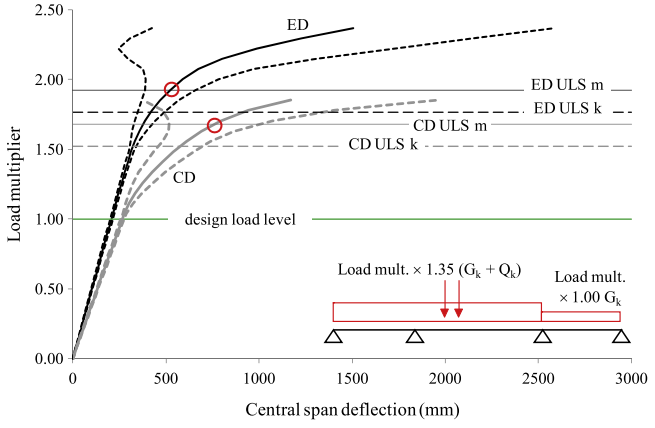

Fig. 10. Load multiplier versus mid-span deflection of the central span with marked limit states.

3.4. Verification according to the Eurocode safety format

The results of the deterministic and probabilistic analyses are used for the verification of the two bridge designs according to the Eurocode safety format. Eq. (10) is used in the form:

$$M_{\mathrm{Ed}}\left(\gamma_G G_k + \gamma_Q Q_k\right) \leq M_{\mathrm{Rd}}\left(\frac{q_{\mathrm{ud}}}{\gamma_{\mathrm{Rd}}\gamma_O}\right) \tag{11}$$

in which M_{Ed} denotes the bending moment (demand) as computed from nonlinear analysis under the design load (DL), M_{Rd} is the resisting bending moment (capacity) as computed from nonlinear analysis under load $q_{\mathrm{ud}}/(\gamma_{\mathrm{Rd}}\gamma_O)$, and q_{ud} is the applied load when the girder reaches the ultimate limit state (i.e., limit states "ED ULS m", "ED ULS k", "CD ULS m", and "CD ULS k"). In Eq. (11), $\gamma_O = 1.20$, and $\gamma_{\mathrm{Rd}} = 1.06$ for resistance model uncertainty when the mean values of capacity and demand from nonlinear analysis are considered, or $\gamma_{\mathrm{Rd}} = 1.00$ for resistance model uncertainty when the characteristic values of capacity (fractile 0.05) and demand (fractile 0.95) from nonlinear analysis are considered. Results for the verification described above are reported in Table 3. All verifications are satisfied with a 44% margin for the elastic design and 21% margin for the combined design, when the ultimate limit states identified through the characteristic values are considered. For the benchmark example considered in this work, the verifications for limit states "ED ULS k" and "CD ULS k" are more stringent than the verifications for limit states "ED ULS m" and "CD ULS m". In fact, the increment of the ultimate load q_{ud}, when the ultimate limit states based on the mean values are considered, is not compensated by the increment of coefficient γ_{Rd}.

4. Conclusions

This paper presents a simplified framework for nonlinear probabilistic response analysis of continuous steel–concrete composite (SCC) girders. The proposed methodology is based on the First-Order Second-Moment (FOSM) approximation. The computation of the required response sensitivities is performed using the Direct Differentiation Method (DDM). This framework provides a computationally efficient numerical simulation of the behavior of SCC girders, while including the influence of uncertainties of material constitutive parameters.

In this study, two design criteria for continuous SCC girders are compared using the proposed nonlinear probabilistic response analysis framework. The design criteria considered are the elastic design, which employs the elastic resistance of all cross sections, and the combined design, which uses the plastic resistance of the cross sections in the sagging regions and the elastic resistance of the cross sections in the hogging regions. A finite element composite beam model with deformable shear connection is adopted for nonlinear probabilistic response analysis. Results obtained for a realistic three-span continuous SCC road bridge, used as the benchmark problem, show that:

(1) The girder designed with the elastic approach and the girder designed with the combined approach both have an almost global linear behavior under the design loads. In addition, the response uncertainties due to uncertainties in material constitutive parameters are limited under the design loads. In fact, the coefficients of variation of the main response quantities are all below 4%.
(2) When the attainment of the elastic limit of the cross sections at the supports (slender cross sections) is assumed as ultimate limit state, both designs have over-strength factors larger than 1.5, obtained by comparing the fractile 0.05 of the capacity and the fractile 0.95 of the demand. For this specific benchmark example, verifications according to the Eurocode safety format are satisfied for both the elastic and combined designs, using both deterministic and probabilistic results.

Even if the results presented in this work are limited to the benchmark problem considered, the formulation presented here for probabilistic nonlinear response analysis of SCC girders is a general, computationally efficient and relatively simple tool for studying various composite girder behavioral aspects, and for quantifying the influence of uncertainties of material constitutive properties on the numerically simulated response of SCC girders.

Table 3
Verifications according to the Eurocode safety format (DL = design loads).

ULS	q_{ud}/DL	γ_{Rd}	γ_O	$M_{Rd}(q_{ud}/(\gamma_{Rd}\gamma_O))$ (kN m)	$M_{Ed}(DL)$ (kN m)	M_{Rd}/M_{Ed}
ED ULS m	1.925	1.06	1.20	130 267.33	85 339.28	1.53
ED ULS k	1.765	1.00	1.20	124 728.39	86 741.98	1.44
CD ULS m	1.679	1.06	1.20	120 908.97	93 983.28	1.29
CD ULS k	1.520	1.00	1.20	115 254.81	95 141.31	1.21

Acknowledgements

The authors gratefully acknowledge partial support of this research by the Louisiana Board of Regents through the Pilot Funding for New Research (Pfund) Program of the National Science Foundation (NSF) Experimental Program to Stimulate Competitive Research (EPSCoR) under Award No. NSF (2008)-PFUND-86 and by the Longwell's Family Foundation through the Fund for Innovation in Engineering Research (FIER) Program. Opinions expressed in this study are those of the authors and do not necessarily reflect those of the sponsor. The authors also gratefully acknowledge Ms. Melissa G. Schultz for the help kindly provided in proofreading the manuscript.

References

[1] Oehlers D, Bradford MA. Elementary behaviour of composite steel and concrete structural members. Oxford: Butterworth-Heinemann; 1999.
[2] Collings D. Steel concrete composite bridges. London: Thomas Telford; 2005.
[3] Dezi L. Architectural and structural design of short and medium span composite bridges. In: Cruz PJS, Simões da Silva L, Schröter F (editors.), Steel bridges: Advanced solutions and technologies. ECCS. Guimarães (Portugal); 2008. p. 5–14.
[4] Johnson RP, Chen S. Local buckling and moment redistribution in class 2 composite beams. Structural Engineering International 1991;1(4):27–34.
[5] Johnson RP, Huang D. Composite bridge beams with mixed-class cross sections. Structural Engineering International 1995;5(2):96–101.
[6] Dekker NW, Kemp AR, Trinchero P. Factors influencing the strength of continuous composite beams in negative bending. Journal of Constructional Steel Research 1995;34(2–3):161–85.
[7] Nethercot DA, Li TQ, Choo BS. Required rotations and moment redistribution for composite frames and continuous beams. Journal of Constructional Steel Research 1995;35(2):121–63.
[8] Couchman G, Lebet JP. A new design method for continuous composite beams. Structural Engineering International 1996;6(2):96–101.
[9] White DW, Barth KE. Strength and ductility of compact-flange I-girders in negative bending. Journal of Constructional Steel Research 1998;45(3): 241–80.
[10] Fabbrocino G, Manfredi G, Cosenza E. Ductility of composite beams under negative bending: An equivalence index for reinforcing steel classification. Journal of Constructional Steel Research 2001;57(2):185–202.
[11] Lääne A, Lebet JP. Design of slender composite bridges considering available support region rotation capacity. Structural Engineering International 2005; 15(2):105–12.
[12] Chen S, Jia Y. Required and available moment redistribution of continuous steel–concrete composite beams. Journal of Constructional Steel Research 2008;64(2):167–75.
[13] European Committee for Standardization. Eurocode 4: Design of composite steel and concrete structures—Part 1–1: General rules and rules for buildings. EN 1994-1-1; December 2004.
[14] European Committee for Standardization. Eurocode 4: Design of composite steel and concrete structures—Part 2: General rules and rules for bridges. EN 1994-2; October 2005.
[15] Melchers RE. Structural reliability analysis and predictions. 2nd ed. Chichester (UK): Wiley; 1999.
[16] Liu JS. Monte Carlo strategies in scientific computing. New York: Springer-Verlag; 2001.
[17] Kleiber M, Antunez H, Hien TD, Kowalczyk P. Parameter sensitivity in nonlinear mechanics: Theory and finite element computations. New York: Wiley; 1997.
[18] Ang AHS, Tang WH. Probability concepts in engineering. 2nd ed. New York: Wiley; 2007.
[19] Zhang Y, Der Kiureghian A. Dynamic response sensitivity of inelastic structures. Computer Methods in Applied Mechanics and Engineering 1993; 108(1–2):23–36.
[20] Conte JP, Vijalapura PK, Meghella M. Consistent finite element response sensitivities in seismic reliability analysis. Journal of Engineering Mechanics 2003;129(12):1380–93.
[21] Conte JP, Barbato M, Gu Q. Finite element response sensitivity, probabilistic response and reliability analyses. Papadrakakis M, Charmpis DC, Tsompanakis Y, Lagaros ND, editors. Computational structural dynamics and earthquake engineering, vol. 2. Oxford (UK): Taylor and Francis; 2008. p. 21–42.
[22] Barbato M. Finite element response sensitivity, probabilistic response and reliability analyses of structural systems with applications to earthquake engineering. Ph.D. thesis. San Diego: University of California; 2007.
[23] Barbato M, Gu Q, Conte JP. Probabilistic push-over analysis of structural and soil-structure systems. Journal of Structural Engineering. 2009 (under review).
[24] Dall'Asta A, Zona A. Non-linear analysis of composite beams by a displacement approach. Computers and Structures 2002;80(27–30):2217–28.
[25] Dall'Asta A, Zona A. Comparison and validation of displacement and mixed elements for the non-linear analysis of continuous composite beams. Computers and Structures 2004;82(23–26):2117–30.
[26] Dall'Asta A, Zona A. Finite element model for externally prestressed composite beams with deformable connection. Journal of Structural Engineering 2005; 131(5):706–14.
[27] Zona A, Barbato M, Conte JP. Nonlinear seismic response analysis of steel–concrete composite frames. Journal of Structural Engineering 2008; 134(6):986–97.
[28] Dall'Asta A, Ragni L, Zona A. Steel–concrete composite beams prestressed by external tendons: Effects of material and geometric nonlinearities. International Journal of Advanced Steel Construction 2006;2(1):53–70.
[29] Zona A, Barbato M, Conte JP. Finite element response sensitivity analysis of steel–concrete composite beams with deformable shear connection. Journal of Engineering Mechanics 2005;131(11):1126–39.
[30] Zona A, Barbato M, Conte JP. Finite element response sensitivity analysis of continuous steel–concrete composite girders. Steel and Composite Structures 2006;6(3):183–202.
[31] Zona A, Barbato M, Conte JP. Finite element response sensitivity analysis of steel–concrete composite structures. Report SSRP-04/02. San Diego: Department of Structural Engineering, University of California; 2004.
[32] Barbato M, Zona A, Conte JP. Probabilistic response analysis of steel–concrete composite structures. In: Voyiadjis G, (editors.), Proceedings of the first American academy of mechanics conference. 2008. CD-ROM.
[33] Menegotto M, Pinto PE. Method of analysis for cyclically loaded reinforced concrete plane frames including changes in geometry and nonelastic behavior of elements under combined normal force and bending. In: Proceedings of the IABSE symposium. 1973. p. 112–23.
[34] Filippou FC, Popov EP, Bertero VV. Effects on bond deterioration on hysteretic behavior of reinforced concrete joints. Report EERC 83-19. Berkeley: Earthquake Engineering Research Center, University of California; 1983.
[35] Barbato M, Conte JP. Finite-element structural response sensitivity and reliability analyses using smooth versus non-smooth material constitutive models. International Journal of Reliability and Safety 2006;1(1–2):3–39.
[36] Balan TA, Spacone E, Kwon M. A 3D hypoplastic model for cyclic analysis of concrete structures. Engineering Structures 2001;23(4):333–42.
[37] Ollgaard JG, Slutter RG, Fisher JW. Shear strength of stud connectors in lightweight and normal weight concrete. AISC Engineering Journal 1971; 55–64.
[38] European Committee for Standardization. Eurocode 2: Design of concrete structures—Part 1–1: General rules and rules for buildings. EN 1992-1-1; December 2004.
[39] European Committee for Standardization. Eurocode 3: Design of steel structures—Part 1–1: General rules and rules for buildings. EN 1993-1-1; May 2005.
[40] European Committee for Standardization. Eurocode 2: Design of concrete structures—Part 2: Concrete bridges—Design and detailing rules. EN 1992-2; October 2005.
[41] European Committee for Standardization. Eurocode—Basis of structural design. EN 1990; December 2005.
[42] European Committee for Standardization. Eurocode 1: Actions on structures—Part 1–1: General actions—Densities, self-weight, imposed loads for buildings. EN 1991-1-1; August 2004.
[43] European Committee for Standardization. Eurocode 1: Actions on structures—Part 1-4: General actions—Wind actions. EN 1991-1-4; July 2005.
[44] European Committee for Standardization. Eurocode 1: Actions on structures—Part 1-5: General actions—Thermal actions. EN 1991-1-5; October 2004.
[45] European Committee for Standardization. Eurocode 1: Actions on structures—Part 2: Traffic loads on bridges. EN 1991-2; March 2005.
[46] European Committee for Standardization. Eurocode 3: Design of steel structures—Part 2: Steel Bridges. EN 1993-2; October 2006.
[47] Galambos TV, Ravindra MK. Properties of steel for use in LRFD. Journal of the Structural Division ASCE 1978;104(9):1459–68.
[48] Mirza SA, MacGregor JG. Variability of mechanical properties of reinforcing bars. Journal of the Structural Division ASCE 1979;105(5):921–37.
[49] Mirza SA, MacGregor JG, Hatzinikolas M. Statistical descriptions of strength of concrete. Journal of the Structural Division ASCE 1979;105(6):1021–37.
[50] Ubejd Mujagić JR, Easterling WS. Reliability assessment of composite beams. Journal of Constructional Steel Research 2009;65(12):2111–28.
[51] Fabbrocino G, Manfredi G, Cosenza E. Non-linear analysis of composite beams under positive bending. Computer and Structures 1999;70(1):77–89.